The Immunomodulatory Benzodiazepine Bz-423 Inhibits B-Cell Proliferation by Targeting c-Myc Protein for Rapid and Specific Degradation

Thomas B. Sundberg,[1] Gina M. Ney,[1] Chitra Subramanian,[2] Anthony W. Opipari, Jr.,[3] and Gary D. Glick[1]

Departments of [1]Chemistry, [2]Pediatrics, and [3]Obstetrics and Gynecology, University of Michigan, Ann Arbor, Michigan

Abstract

Myc proteins regulate cell growth and are oncogenic in many cancers. Although these proteins are validated molecular anticancer targets, new therapies aimed at modulating myc have yet to emerge. A benzodiazepine (Bz-423) that was discovered in efforts to find new drugs for lupus was found recently to have antiproliferative effects on Burkitt's lymphoma cells. We now show that the basis for the antiproliferative effects of Bz-423 is the rapid and specific depletion of c-myc protein, which is coupled to growth-suppressing effects on key regulators of proliferation and cell cycle progression. c-Myc is depleted as a result of signals coupled to Bz-423 binding its molecular target, the oligomycin sensitivity-conferring protein subunit of the mitochondrial F_1F_o-ATPase. Bz-423 inhibits F_1F_o-ATPase activity, blocking respiratory chain function and generating superoxide, which at growth-inhibiting concentrations triggers proteasomal degradation of c-myc. Bz-423-induced c-myc degradation is independent of glycogen synthase kinase but is substantially blocked by mutation of the phosphosensitive residue threonine 58, which when phosphorylated targets c-myc for ubiquitination and subsequent proteasomal degradation. Collectively, this work describes a new lead compound, with drug-like properties, which regulates c-myc by a novel molecular mechanism that may be therapeutically useful. (Cancer Res 2006; 66(3): 1775-82)

Introduction

The proto-oncogene c-myc is a basic helix-loop-helix leucine zipper (bHLHZip) transcription factor with a fundamental role in many normal cellular processes, including the G_1-S-phase cell cycle transition (1). c-Myc activates or represses transcription of target genes by either binding to specific DNA elements as a heterodimer with Max, another bHLHZip protein, or forming complexes with other transcription factors, such as Sp1 (2–4).

Genetic alterations that affect c-myc, such as point mutations, amplification, or translocation, convey oncogenic properties (5). As many as 70,000 cancer deaths per year in the United States can be attributed to deregulation of this protein (6). Burkitt's lymphoma, a cancer of B cells, is specifically caused by increased c-myc expression. In Burkitt's lymphoma, c-myc is constitutively overexpressed as a result of translocation of c-myc to the immunoglobulin gene locus, placing it under the transcriptional control of immunoglobulin enhancers (7). Experimental strategies to reduce c-myc expression or disrupt its function in Burkitt's lymphoma cells have successfully treated Burkitt's lymphoma in mice (8, 9).

Bz-423 is a novel benzodiazepine that induces either apoptotic or antiproliferative responses in normal and transformed lymphoid cells (10, 11). The apoptotic activity against lymphoid cells accounts for its therapeutic effects against lupus and arthritis in mice (10, 12). The target of Bz-423 and its apoptotic mechanism have been elucidated. Bz-423 binds to the oligomycin sensitivity-conferring protein (OSCP) component of the mitochondrial F_1F_o-ATPase and inhibits ATP synthesis, which blocks electron transport and leads to superoxide (O_2^-) production via a respiratory state 3 to state 4 transition (13). O_2^- produced in this manner functions as a second messenger that activates a tightly regulated apoptotic signaling pathway (10). The amount of O_2^- produced following inhibition of the F_1F_o-ATPase by Bz-423 is concentration dependent. Concentrations of Bz-423 below those required to kill cells produce proportionally less O_2^- and cause Burkitt's lymphoma cells to stop proliferating due to cell cycle arrest at the G_1 checkpoint (11).

Prior studies showed that pretreating cells with antioxidants restores normal proliferation, which links Bz-423-induced O_2^- with growth arrest (11). Based on this finding, the experiments described here were done to probe the molecular basis for the antiproliferative effects of Bz-423 in Burkitt's lymphoma cells. Our results show that Bz-423 rapidly depletes Burkitt's lymphoma cells of c-myc protein in a O_2^- dependent manner. c-Myc protein stability seems to be reduced by a post-translational mechanism because no change in the level of c-myc transcript is observed, inhibition of proteasome activity blocks the decrease, and mutation of specific residues involved in proteolytic processing blocks the effects of Bz-423 on both c-myc and growth inhibition. Collectively, these results identify a unique mechanism to regulate c-myc and suggest that Bz-423 may have activity against malignant diseases associated with deregulated myc expression.

Materials and Methods

Reagents. Manganese(III) *meso*-tetrakis(4-benzoic acid)porphyrin (MnTBAP) was purchased from Alexis Corp. (San Diego, CA). D,L-α-Difluoromethylornithine (DFMO), trichloroacetic acid (TCA), L-ornithine, SB-216763, and SB-415286 were purchased from Sigma-Aldrich (St. Louis, MO). Bortezomib was provided by V. Castle (University of Michigan). Bz-423 was synthesized as described previously and applied to cellular medium in aqueous DMSO (14), such that DMSO was present at a final concentration of 0.5% (v/v) in all experiments.

Note: Supplementary data for this article are available at Cancer Research Online (http://cancerres.aacrjournals.org/).

Requests for reprints: Anthony W. Opipari, Jr., Division of Gynecologic Oncology, Department of Obstetrics and Gynecology, University of Michigan, 1500 East Medical Center Drive, L4000 Women's Hospital, Ann Arbor, MI 48109. Phone: 734-764-9106; Fax: 734-615-8902; E-mail: aopipari@umich.edu.

doi:10.1158/0008-5472.CAN-05-3476

Cell culture and transfections. Ramos B cells were purchased from American Type Culture Collection (Manassas, VA). Cells (10^6/mL) were maintained in RPMI 1640 (Mediatech, Herndon, VA) as described previously (10). pcDNA3-c-myc, an expression vector containing Flag-tagged human c-myc, was used for transfection. Mutation of threonine 58 (T58) and serine 62 (S62) in the pcDNA3-c-myc coding sequence was done using the QuickChange II XL Site-Directed Mutagenesis kit (Stratagene, La Jolla, CA) according to the manufacturer's protocol. Briefly, synthetic DNA primers (5′-GAGCTGCTGCCCGCTCCGCCCCTGTCCCCT-3′ and 5′-AGGGGACAGGGGCGGAGCGGGCAGCAGCTC-3′ for c-myc^{T58A}, 5′-ACCCCGCCCCTGGCACCTAGCCGCCGC-3′ and 5′-GCGGCGGCTAGGTGCCAGGGGCGGGGT-3′ for c-myc^{S62A}, and GAGCTGCTGCCCGCTCCGCCCCTGGCACCTAGCCGCCGC-3′ and 5′-GCGGCGGCTAGGTGCCAGGGGCGGAGCGGGCAGCAGCTC-3′ for c-myc$^{T58A/S62A}$) were used in PCR with the template plasmid. For transfection into Ramos cells, 7.5×10^6 cells were electroporated with an Amaxa Nucleofector apparatus (Gaithersburg, MD) according to the manufacturer's protocol. After 24 hours, stably transfected cells were selected and maintained in RPMI 1640 containing geneticin (1.5 mg/mL; Life Technologies, Rockville, MD).

Gene expression profile. RNA was isolated from replicate samples of Ramos cells treated with Bz-423 ($n = 2$) or vehicle control ($n = 4$) for 4 hours using a RNeasy mini kit (Qiagen, Inc., Valencia, CA) and hybridized to HGU133A Affymetrix Gene Chips. Expression data were evaluated to identify genes with >2-fold change in expression with $P < 0.01$.

Measurement of ornithine decarboxylase activity. Ornithine decarboxylase (ODC) activity in Ramos cells treated with either Bz-423 or vehicle control was evaluated as described previously (15). ODC activity, quantified as the amount of [^{3}H]putrescine produced from [^{3}H]ornithine, was normalized to cellular protein content.

Measurement of cellular polyamines. Cellular polyamine content in Ramos cells treated with either Bz-423 or vehicle control was measured by reverse-phase high-performance liquid chromatography (RP-HPLC) using a Spherisorb C_{18} S3 ODS2 column (15 × 0.46 cm i.d.; 3 μm particle size; Waters Corp., Milliford, MA) as described previously (16).

Immunoblotting. Cells were lysed by resuspension in four times packed cell volume of lysis buffer as described previously (10). Lysates were separated by SDS-PAGE, transferred to polyvinylidene difluoride membranes, and incubated with primary antibodies for proteins of interest, including ODC (29), Flag (M2), and β-tubulin (TUB2.1) purchased from Sigma-Aldrich. The ODC antizyme 1 (OAZ1) antibody (PW 8885) was purchased from Biomol International (Plymouth Meeting, PA). Antibodies for phospho-c-myc (T58/S62), cyclin-dependent kinase (CDK) 6 (DCS-83), retinoblastoma protein (pRb; 4H1), phospho-Rb (S780), phospho-Rb (S795), and phospho-Rb (S807/811) were purchased from Cell Signaling Technology (Beverly, MA). Antibodies for c-myc (9E10), β-catenin (14), p27^{Kip1} (G17-524), p21^{Cip1} (SX118), cyclin D1 (DCS-9), cyclin D2 (G132-43), cyclin D3 (G107-565), cyclin E (HE12), CDK2 (55), and CDK4 (DCS-35) were purchased from BD PharMingen (San Jose, CA). Primary antibodies were detected using horseradish peroxidase–linked donkey anti-rabbit IgG or sheep anti-mouse IgG (Amersham Biosciences, Little Chalfont, Buckinghamshire, United Kingdom) and visualized by the enhanced chemiluminescence detection system (Amersham Biosciences). Protein levels were estimated by densitometry and normalized with respect to β-tubulin, which was used as a loading control.

RNA analyses. RNA was isolated from Ramos cells treated with Bz-423 or vehicle control using a RNeasy mini kit. Semiquantitative reverse transcription-PCR (RT-PCR) was done as described (17) using the following primers: ODC (forward GAGCACATCCCAAAGCAAAGT and reverse TCCAGAGTCTGACGGAAAGTA), OAZ1 (forward AGCAGTGAGAGTTCCAGGGTC and reverse ACTGCAAAGCTGTCCTTGCTC), c-Myc (forward TTCGGGTAGTGGAAAACCAG and reverse CAGCAGCTCGAATTTCTTCC), and β-actin (forward TGGCATTGTTACCAACTGGGACG and reverse GCTTCTCTTTGATGTCACGCAQCG). β-Actin was used as an internal standard for RNA normalization, and expression patterns were determined from two separate experiments.

Assessment of DNA content by flow cytometry. DNA content was assessed by incubating cells in labeling solution (50 μg/mL propidium iodide in PBS containing 0.2% Triton X-100 and 10 μg/mL RNase A) for 24 hours followed by analysis with a FACSCalibur flow cytometer equipped with CellQuest software (BD Immunocytometry, San Diego, CA).

Measurement of growth inhibition. Growth inhibition of wild-type and c-myc-overexpressing Ramos cells was quantified using the sulforhodamine B assay as described previously (18).

Results

Bz-423 modulates cellular polyamine metabolism. Prior studies showed that Bz-423 specifically blocks the cell cycle at the G_1-S transition, which is regulated by a complex network of signals, some of which are controlled at the transcriptional level (11). Consequently, genome-wide cDNA microarray analysis was used to screen for Bz-423-induced changes in mRNA expression to identify potential responses coupling Bz-423 to G_1 arrest. For this experiment, RNA was isolated from Bz-423-treated Ramos cells (a Burkitt's lymphoma–derived cell line possessing a germinal center phenotype; ref. 19) and changes in gene expression at 4 hours were examined. Bz-423 significantly increased expression of several genes, including those that encode proteins involved in energy production and the stress response (Supplementary Table S1). These changes are not surprising based on the target of Bz-423, the F_1F_o-ATPase, a key enzyme in cellular energy production. Unexpectedly, this analysis also showed that OAZ1 was significantly induced (Supplementary Table S1). OAZ1 depletes cellular polyamines by specifically inhibiting ODC, an enzyme that catalyzes the conversion of ornithine to putrescine, a rate-controlling step in polyamine biosynthesis (20). This finding suggests that Bz-423 might alter polyamine metabolism. Polyamines are required for normal cell growth, and severe depletion blocks proliferation and causes cell death (21). Therefore, we hypothesized that Bz-423 induces G_1 arrest by altering cellular polyamine metabolism.

To test this hypothesis, we determined if Bz-423 reduces ODC activity by measuring the amount of [^{3}H]putrescine Ramos cells produced using [^{3}H]ornithine as a substrate in the presence of Bz-423 or vehicle alone as described previously (15). As expected, Bz-423 reduced apparent ODC activity within 4 hours to a similar extent as DFMO, a specific inhibitor of ODC (ref. 21; Fig. 1*A*). Based on the induction of OAZ1 gene expression and the observed decrease in ODC activity, we predicted that Bz-423 decreased ODC activity and protein levels by a post-translational mechanism involving OAZ1-dependent inhibition and subsequent proteolytic degradation. As such, Bz-423 was expected to decrease ODC protein but not affect ODC mRNA levels. To evaluate this hypothesis, Ramos cells were treated with Bz-423, and lysates were analyzed by immunoblotting and RT-PCR to measure ODC and OAZ1 protein and mRNA levels. As predicted, growth-inhibitory concentrations of Bz-423 substantially reduced levels of ODC protein by 8 hours (Fig. 1*B*). Unexpectedly, however, Bz-423 significantly decreased ODC mRNA levels by 3 hours, whereas OAZ1 protein and mRNA levels were *unchanged* over the same period (Fig. 1*B*). Taken together, these findings suggest that OAZ1 does not mediate the decrease in ODC protein.

To determine if the decrease in ODC protein and activity caused by Bz-423 actually resulted in decreased cellular polyamine levels, Ramos cells were treated with Bz-423 and lysed with TCA, and acid-soluble polyamines were analyzed by RP-HPLC as described previously (16). Bz-423 reduced polyamine levels and the magnitude of this effect was similar to the reduction caused by DFMO (Fig. 1*C*). Analyzing the change in polyamine levels as a

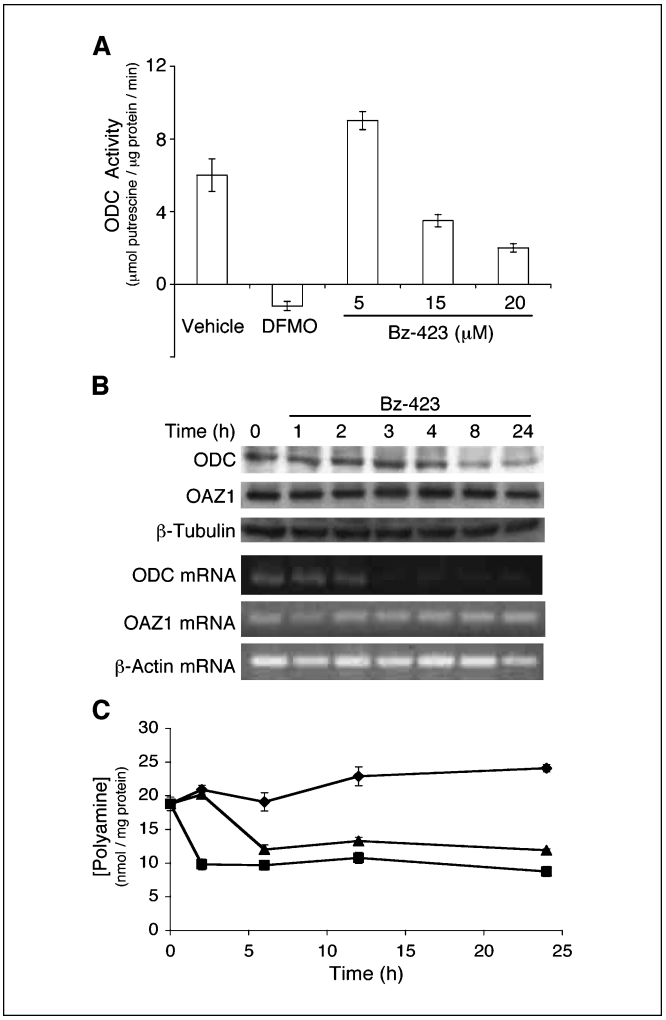

Figure 1. Effect of Bz-423 on polyamine metabolism. *A,* Ramos cells were treated with either DFMO (1 mmol/L) or Bz-423 (indicated concentration) and ODC activity was determined as the amount of [^{3}H]putrescine produced from [^{3}H]ornithine. *B,* whole-cell lysates or RNA were isolated from Ramos cells treated with Bz-423 (15 μmol/L) for indicated times and immunoblots or RT-PCR were done to detect ODC and OAZ1 protein or mRNA, respectively. *C,* Ramos cells were treated with vehicle control (♦), DFMO (1 mmol/L; ■), or Bz-423 (15 μmol/L; ▲) and polyamine levels were determined by RP-HPLC.

function of time indicates that polyamine depletion corresponds with the reduction in ODC protein. Collectively, these findings suggest that Bz-423-induced growth arrest may be linked to its effects on ODC and changes in cellular polyamines.

Bz-423 decreases c-Myc and modulates expression of cell cycle regulatory proteins. The absence of an effect of Bz-423 on OAZ1 protein argues against a mechanism whereby Bz-423 targets ODC for proteasomal degradation by a post-translational mechanism. Moreover, the decrease in ODC mRNA suggests that Bz-423 might affect the transcriptional activity of the *odc* gene. c-Myc is the principal transcriptional activator of *odc*, and there are two high-affinity c-myc-binding sites within the first intron of the *odc* gene (22). Therefore, we hypothesized that Bz-423 might reduce c-myc expression or activity to account for the observed changes in *odc* mRNA and potentially its affects on cell proliferation. Consistent with this expectation, immunoblots of lysates from Ramos cells treated with Bz-423 showed that c-myc protein was decreased significantly by 4 hours and by >90% after 24 hours (Fig. 2).

Besides transcriptional activation of *odc*, c-myc promotes the G_1-S transition by acting as both a transcriptional activator and a repressor to coordinate expression of cell cycle regulatory genes (1, 6). Cell cycle progression is directed by CDKs, whose activity is regulated by the relative levels of cyclins and CDK inhibitors (CDKI; ref. 23). In particular, active complexes of CDK2, CDK4, or CDK6 with D-type cyclins as well as complexes of cyclin E and CDK2 promote the G_1-S transition. Cyclin-CDK complexes are inhibited by CDKIs $p21^{Cip1}$ and $p27^{Kip1}$ (24). c-Myc activates transcription of CDK2, CDK4, and CDK6 as well as D- and E-type cyclins and represses transcription $p21^{Cip1}$ and $p27^{Kip1}$ (25). Because Bz-423 rapidly decreased c-myc protein levels, we expected to also find increased expression of the CDKIs and decreased expression of CDK2, CDK4, and CDK6 as well as D- and E-type cyclins.

In Bz-423-treated Ramos cell lysates, CDK4 decreased to <20% of basal levels (within 2 hours of treatment) and expression of CDK2 and CDK6 was reduced after 8 hours. Cyclin D3 and E were reduced by Bz-423, whereas cyclin D1 and D2 remained constant over the same period. In untreated Ramos cells, cyclin D3 seemed to be expressed at a significantly greater level than either cyclin D1 or cyclin D2 (data not shown), indicating that in Ramos cells cyclin D3 is the predominant D-type cyclin. $p21^{Cip1}$ was barely detectable in untreated Ramos cells and did not increase after Bz-423 treatment. Finally, Bz-423 induced a small but significant increase in $p27^{Kip1}$ by 24 hours (Fig. 2). Collectively, these results indicate that Bz-423 alters expression of cell cycle regulatory genes in a

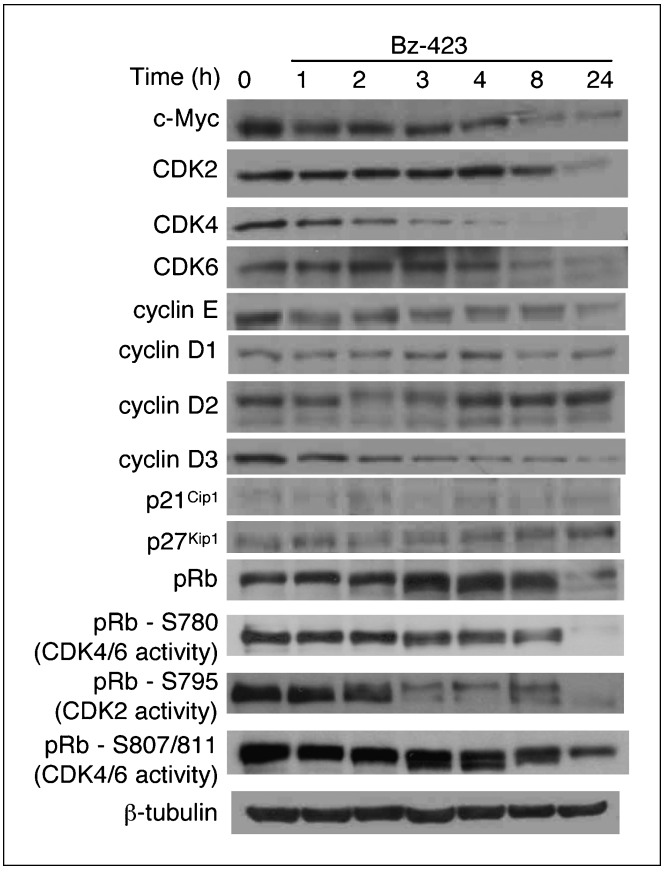

Figure 2. Bz-423 alters c-myc protein levels, expression of cell cycle regulatory genes, and phosphorylation of pRb. Whole-cell lysates were isolated from Ramos cells treated with Bz-423 (15 μmol/L) for indicated times and immunoblots were done with specific antibodies.

pattern consistent with the observed decrease in c-myc protein and G_1 cell cycle arrest.

The primary substrates of the CDKs are the pRb family of pocket proteins (pRb, p107, and p130; ref. 26). In their hypophosphorylated state, pocket proteins bind to members of the E2F family of transcription factors, preventing transcription of E2F-regulated genes that drive S-phase entry. Phosphorylation of the pocket proteins by CDKs results in derepression of E2F-dependent gene transcription and progression through the G_1-S checkpoint (26). Bz-423 reduces expression of D- and E-type cyclins as well as CDK2, CDK4, and CDK6. Consequently, Bz-423 was expected to decrease the levels of phosphorylated pRb, p107, and p130. In untreated Ramos cells, pRb is highly expressed, whereas p107 and p130 are barely detectable (data not shown). Following treatment with Bz-423, the phosphorylation state of pRb decreased as shown by an increase in its mobility on SDS-PAGE (Fig. 2). In G_1, complexes of D-type cyclins with either CDK2 or CDK4 phosphorylate serine residues located throughout pRb, including S780, S795, S807, and S811 (27). Cyclin E-CDK2 complexes phosphorylate a subset of these residues, including S795, during the passage through the G_1-S checkpoint (27). Phospho-Rb antibodies specific for S780, S795, and S807/S811 were used to assess the *in vivo* activities of CDK2, CDK4, and CDK6 (28). The results of immunoblotting with these antibodies were consistent with decreased CDK2, CDK4, and CDK6 activities corresponding to the Bz-423-induced decrease in expression of these CDKs (Fig. 2). In summary, Bz-423 alters expression of cell cycle regulatory genes resulting in diminished pRb phosphorylation and decreases ODC expression and cellular polyamine levels. In Ramos cells, inhibition of either ODC, with the specific inhibitor DFMO (ref. 21; GI_{50}, 0.61 ± 0.07 mmol/L), or the CDK2-cyclin E complex, with roscovitine (GI_{50}, 14 ± 2 μmol/L; ref. 29), causes growth arrest. Thus, Bz-423-induced growth arrest is mediated by two paths, decreased polyamines and pRb phosphorylation, either of which independently blocks proliferation.

O_2^- mediates the Bz-423-induced decrease in c-Myc and downstream effects on polyamine metabolism. The manganese superoxide dismutase mimetic, MnTBAP, scavenges Bz-423-induced O_2^- and blocks the subsequent effects on cell proliferation or viability (10, 11). Consequently, we predicted this antioxidant would prevent the decrease in c-myc as well as the drop in ODC expression and depletion of cellular polyamines induced by Bz-423 if these responses were coupled to Bz-423 binding to the OSCP target via a O_2^- signal. To test this predicted linkage, Ramos cells were pretreated with MnTBAP and then incubated with Bz-423. MnTBAP prevented the decrease in c-myc protein levels as well as the drop in ODC protein and mRNA (Fig. 3*A*). MnTBAP also prevented the Bz-423-induced reduction in ODC activity and maintained normal polyamine levels (Fig. 3*B* and *C*). Next, we treated cells with other agents that increase reactive oxygen species to determine if the O_2^- induced by Bz-423 is sufficient to reduce c-myc levels. Ramos cells were treated with hydrogen peroxide, *t*-butyl hydroperoxide, and arsenic trioxide (As_2O_3), an agent that generates O_2^- by targeting mitochondrial function (30). Interestingly, whereas neither hydrogen peroxide nor *t*-butyl hydroperoxide affected c-myc levels (data not shown), As_2O_3 reduced c-myc to a similar extent as Bz-423 (Fig. 3*D*). These data indicate that a specific relationship may exist between mitochondrially derived O_2^- and the pathway leading to rapid c-myc degradation and that

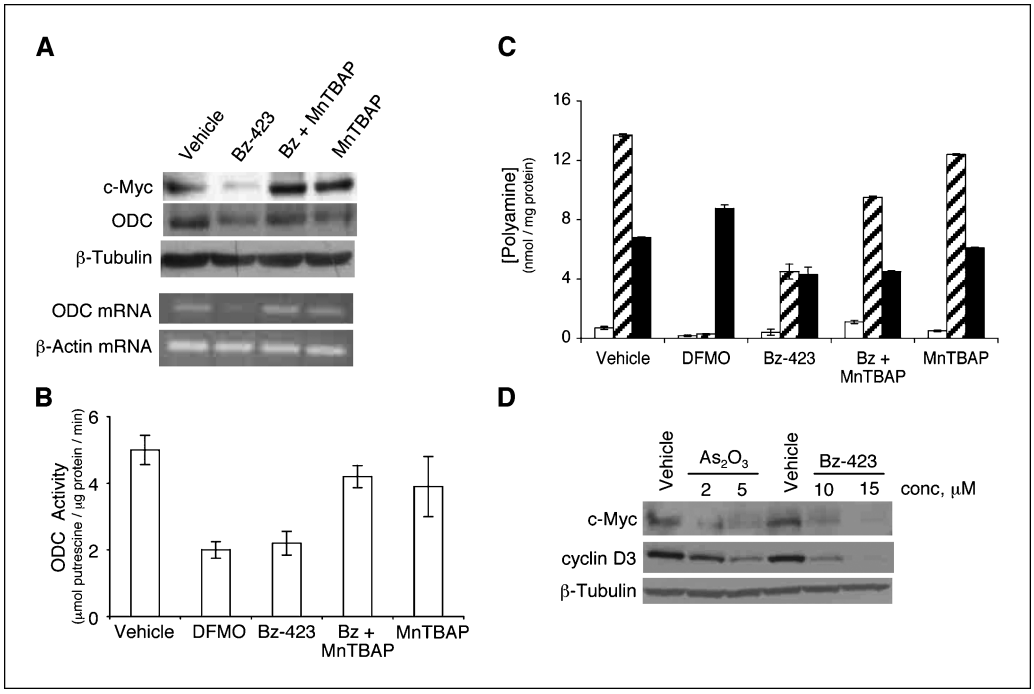

Figure 3. Bz-423-induced O_2^- mediates the decrease in c-myc protein, ODC expression, and polyamine levels. *A,* whole-cell lysates or RNA were prepared from Ramos cells pretreated with MnTBAP (100 μmol/L) and then treated with Bz-423 (15 μmol/L) for 8 hours. Immunoblotting and RT-PCR were done to evaluate c-myc and ODC protein and mRNA levels, respectively. *B,* Ramos cells were treated with DFMO (1 mmol/L) for 4 hours or pretreated with MnTBAP (100 μmol/L) and then treated with Bz-423 (15 μmol/L) for 4 hours and ODC activity was determined as the amount of [^{3}H]putrescine produced from [^{3}H]ornithine. *C,* Ramos B cells were treated with DFMO (1 mmol/L) for 36 hours or pretreated with MnTBAP (100 μmol/L) and then treated with Bz-423 (15 μmol/L) for 24 hours and concentrations of the polyamines putrescine (*white columns*), spermidine (*hatched columns*), and spermine (*black columns*) were determined by RP-HPLC. *D,* whole-cell lysates were prepared from Ramos cells treated with either Bz-423 (indicated concentrations) or As_2O_3 (indicated concentrations) for 6 hours and immunoblotted with specific antibodies for proteins of interest.

this is not recapitulated by treatment with exogenous oxidants. Collectively, these results couple binding of Bz-423 to its cellular target, O_2^- generation, and reduction in c-myc with subsequent effects on polyamine metabolism and transcription.

Bz-423 depletes c-Myc by a mechanism that involves the 26S proteasome. *c-Myc* expression is tightly regulated at the transcriptional and post-translational levels through processes that control mRNA and protein stability (31). To determine if Bz-423 decreases c-myc protein by a mechanism involving either transcription or mRNA stability, RNA was isolated from Bz-423-treated Ramos cells, and steady-state *c-myc* mRNA levels were measured using semiquantitative RT-PCR. As seen in Fig. 4*A*, c-myc RNA levels remained essentially unchanged for 8 hours with a slight drop only after 24 hours of treatment. In contrast, c-Myc protein expression dropped significantly within 4 hours and by >90% after 24 hours (Fig. 4*A*). Thus, *c-myc* transcript levels remain stable during the period in which c-myc protein levels precipitously drop, arguing that the Bz-423-induced decrease in c-myc protein occurs by a process that affects either protein translation or stability.

The stability of c-myc protein is reduced by agents and conditions that affect cell growth and is regulated through mechanisms that ultimately control ubiquitin-mediated degradation by the 26S proteasome (32–34). Highly conserved NH_2-terminal residues 45 to 63, known as the myc box 1 (MB1), are critical for ubiquitin-mediated c-myc degradation (35). Within MB1, S62 and T58 are phosphorylated by extracellular signal-related kinases and glycogen-synthase kinase 3β (GSK-3β), respectively (34). Phosphorylation of S62 initially stabilizes c-myc protein (34) but also primes it for subsequent T58 phosphorylation by GSK-3β, which triggers degradation of c-myc through the ubiquitin-proteasome pathway (36, 37).

We expected the Bz-423-induced decrease in c-myc might result from increased proteasomal degradation and predicted that the phosphosensitive residue T58 was involved. To test this hypothesis, we treated Ramos cells with Bz-423 together with bortezomib, a dipeptidyl boronic acid inhibitor of the 26S proteasome (38). Blocking proteasome function in Ramos cells by pretreating with bortezomib before incubation with Bz-423 prevented the decreases in c-myc and cyclin D3, one of the c-myc-dependent gene products affected by Bz-423 (Fig. 4*B*).

Having identified a role for the proteasome in Bz-423-mediated degradation of c-myc, we stably transfected Ramos cells to express Flag epitope-tagged wild-type c-myc and c-myc mutants in which T58, S62, or both residues were substituted with alanine. We generated these cells to test whether Bz-423-induced c-myc degradation required these specific *cis*-acting MB1 elements commonly involved in ubiquitin-mediated proteolysis. In addition, if the mutation of T58 prevented Bz-423-induced c-myc degradation, cells transfected with this mutant construct would allow us to determine if the decrease in c-myc was necessary for Bz-423-induced growth inhibition and cell cycle arrest.

When stably transfected cells expressing these proteins were exposed to Bz-423, the levels of Flag-tagged wild-type c-myc and the c-myc^{S62A} mutant decreased in a time course similar to the decrease of endogenous c-myc in cells transfected with a vector control (Fig. 5*A*). As predicted above, the c-myc^{T58A} mutant and the double mutant c-myc$^{T58A/S62A}$ proteins were substantially resistant to Bz-423-induced degradation at all times and concentrations tested, relative to transfected wild-type c-myc and endogenous c-myc in vector control cells (Fig. 5*A*). From these results, we conclude that T58 is critical for Bz-423-induced degradation of c-myc.

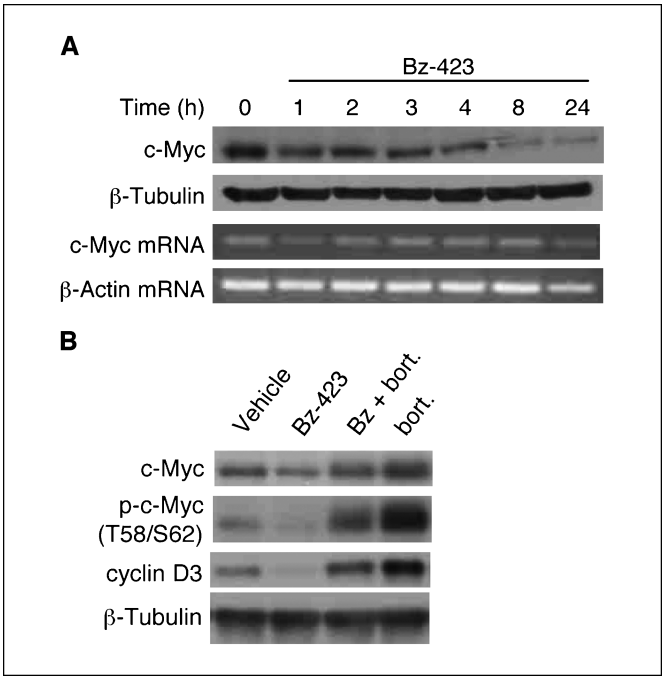

Figure 4. Bz-423 decreases c-myc protein by a mechanism involving proteasomal degradation. *A,* Ramos cells were treated with Bz-423 (15 μmol/L), whole-cell lysates or RNA were isolated, and immunoblots or RT-PCR were done as indicated. *B,* whole-cell lysates were prepared after Ramos cells were pretreated with the bortezomib (*bort.*; 2.5 μmol/L) and then incubated with Bz-423 (15 μmol/L) for 6 hours. Immunoblots were done with specific antibodies as indicated.

We next evaluated the clones expressing the wild-type and mutant c-myc proteins to determine their sensitivity to Bz-423-induced growth inhibition and cell cycle arrest. After treatment with Bz-423 for 48 hours, the GI_{50} was significantly increased in c-myc^{T58A}- and c-myc$^{T58A/S62A}$-expressing cells (15.6 ± 1.4 and 15.8 ± 0.6 μmol/L, respectively) compared with cells expressing wild-type c-myc (11.0 ± 0.9 μmol/L), whereas the GI_{50} for c-myc^{S62A}-expressing cells (12.9 ± 1.4 μmol/L) increased only moderately. When these cells were analyzed to determine the distribution of cells across the cell cycle, the wild-type c-myc and c-myc^{S62A} cells showed G_1 arrest as observed previously in Ramos cells treated with Bz-423 (Fig. 5*B*). However, c-myc^{T58A}- and c-myc$^{T58A/S62A}$-expressing cells showed no significant difference in cell cycle distribution compared with vehicle-treated cells (Fig. 5*B*). These findings indicate that the decrease in c-myc in response to Bz-423 is a necessary part of the mechanism that leads to growth arrest in Burkitt's lymphoma cells.

Because T58 phosphorylation promotes ubiquitin-mediated proteasomal degradation, it is possible that Bz-423 is acting to induce increased T58 phosphorylation to trigger c-myc degradation. To explore this possibility, Bz-423-treated cells were immunoblotted with anti-phospho-c-myc (T58/S62), which recognizes c-myc either singly phosphorylated at T58 or doubly phosphorylated at T58 and S62. This antibody does not bind to singly phosphorylated S62 or unphosphorylated c-myc (34, 36). Surprisingly, no increase in phospho-c-myc species detected by this antibody was observed. Instead, the c-myc phosphoprotein levels decreased with identical kinetics to total c-myc protein (Fig. 6*A*). As a control, lysates were also prepared from Ramos cells following B-cell receptor stimulation with anti-IgM (28, 33). When these activated cells were immunoblotted for total and T58 phosphorylated c-myc, an initial accumulation of both c-myc and

phospho-c-myc (T58/S62) was seen, with a maximum reached at 4 hours followed by a decrease in both species to sub-basal levels by 24 hours (Fig. 6*A*). The absence of an early increase in phosphospecies induced by Bz-423 argues that the decrease in c-myc does not involve a mechanism that increases T58 phosphorylation.

A described above, GSK-3β phosphorylates T58 to trigger proteasomal degradation of c-myc in response to stimuli, including serum withdrawal and B-cell receptor ligation (34, 37). The absence of increased levels of T58 phospho-c-myc in response to Bz-423, however, suggests GSK-3β is not involved. To further exclude this possibility, cells were treated with two structurally distinct GSK-3β inhibitors (SB-216763 and SB-415286; ref. 39) before Bz-423. Neither inhibitor prevented the decrease in c-myc or the associated reduction of cyclin D3 caused by Bz-423 (Fig. 6*B*). Effective inhibition of GSK-3β by SB-216763 and SB-415286 was confirmed because c-myc species recognized by anti-phospho-c-myc (T58/S62) were decreased compared with levels in vehicle-treated cells

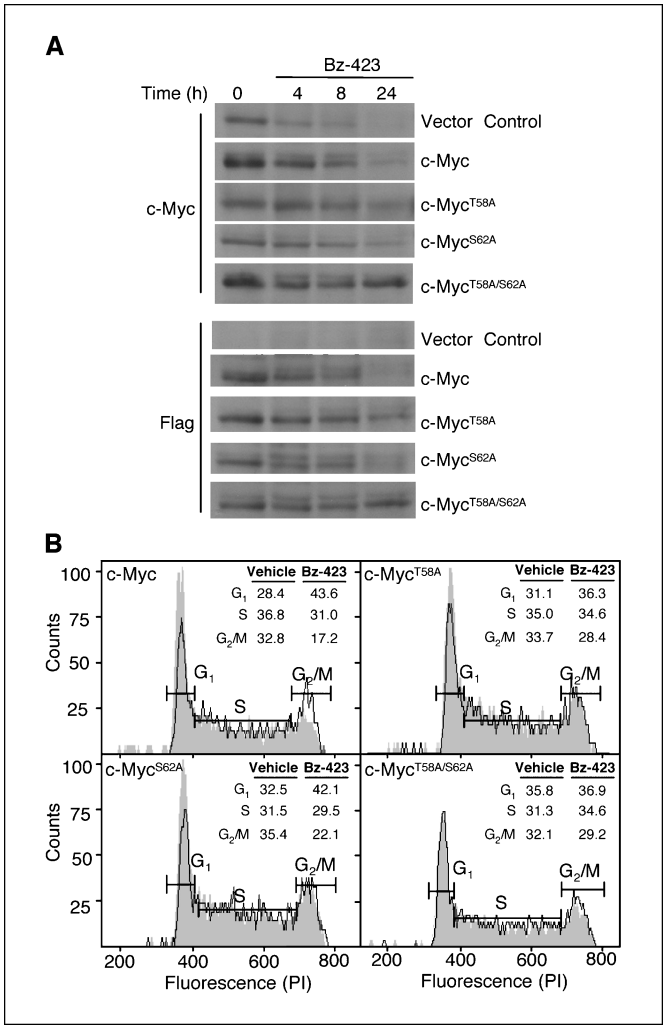

Figure 5. Phosphosensitive residue T58 is critical for Bz-423-induced degradation of c-myc and G_1 arrest. Ramos cells stably expressing Flag epitope-tagged wild-type c-myc or c-myc with alanine substitutions at T58, S62, or both residues were (*A*) treated with Bz-423 (15 μmol/L) and whole-cell lysates were isolated and immunoblots were done as indicated or (*B*) treated with vehicle (*black histogram*) or Bz-423 (15 μmol/L; *gray histogram*) for 24 hours and their cell cycle distributions were determined by propidium iodide staining and flow cytometry. *Inset tables,* percentage of viable cells in the G_1-G_0, S, and G_2-M phases of the cell cycle for each experimental condition.

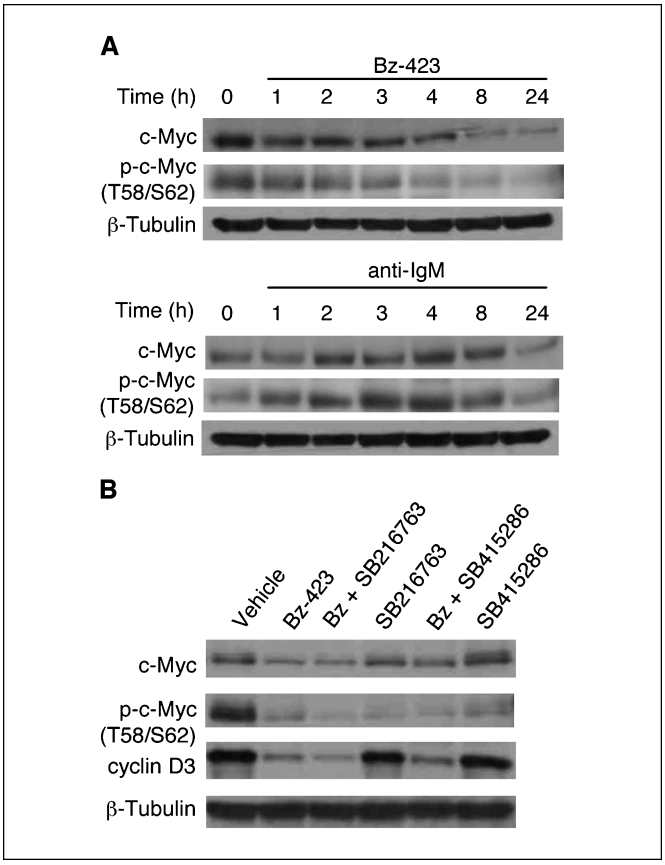

Figure 6. Bz-423 does not increase T58 phosphorylation. *A,* Ramos cells were treated with Bz-423 (15 μmol/L) or anti-IgM (10 μg/mL), after which whole-cell lysates were immunoblotted with specific antibodies as indicated. *B,* whole-cell lysates were isolated from Ramos cells that had been pretreated with the GSK-3β inhibitors SB-216763 (30 μmol/L) or SB-415286 (30 μmol/L) and then incubated with Bz-423 (15 μmol/L) for 6 hours and immunoblots were done with specific antibodies as indicated.

(Fig. 6*B*). Together, these results support an inducible proteolytic pathway to regulate c-myc that involves the proteasome but not increased T58 phosphorylation by GSK-3β. Thus, it is likely that other post-translational modifications on this critical residue, such as glycosylation, are involved.

Discussion

c-Myc drives cellular proliferation by transcriptionally regulating a large number of genes (1). Its effects on proliferation substantially explain why deregulation of c-myc causes neoplastic cell growth and is frequently associated with cancers (1, 5). Strategies to control c-myc expression and/or activity constitute a rational approach to cancer treatment, and proposed approaches include interference with c-myc/Max dimerization and c-myc genetic silencing with small interfering RNAs or peptide-nucleic acid anti-genes (40, 41). Presently, all these strategies remain experimental. Although small-molecule inhibitors of c-myc/Max dimerization have been identified, which prevent or reduce transcriptional activation by c-myc (42, 43), the effectiveness of this particular strategy may be limited because, independent of Max, c-myc can still repress transcription of many genes that block proliferation, such as $p21^{Cip1}$ (4). Thus, a workable strategy to regulate c-myc protein levels has potential to be highly useful, particularly in disease contexts where genetic translocation leads to overexpression. The results presented here show a new

mechanism to reduce c-myc protein levels in Burkitt's lymphoma cells. Antiproliferative concentrations of Bz-423 rapidly deplete c-myc protein and this is followed by the expected consequences on the expression of targets of c-myc transcriptional activation and repression.

In general, c-myc protein stability is determined by the phosphorylation status of key residues within a highly conserved region from residues 45 to 63 known as MB1 (44). Phosphorylation of S62 increases c-myc half-life but also primes the protein for T58 phosphorylation by GSK-3β, which targets c-myc for ubiquitination and proteasomal degradation (45). Our results show that Bz-423 decreases total c-myc and phospho-T58-c-myc with identical kinetics. Because an initial increase in phospho-T58 would be expected if the Bz-423-induced degradation of c-myc was mediated by increased phosphorylation of this residue, we conclude that Bz-423 is not acting by increasing T58 phosphorylation. Moreover, GSK-3β inhibitors did not block the Bz-423-induced decrease in c-myc. This observation further supports our conclusion that inducible T58 phosphorylation is not required for the response and provides direct evidence that GSK-3β is specifically not required.

Nevertheless, cells expressing c-myc with either single alanine substitution at T58 or double substitution of T58 and S62 are resistant to Bz-423-induced changes in cell cycle and are less sensitive to Bz-423-induced growth arrest as evidenced by an increase in the GI_{50} values compared with cells transfected with wild-type c-myc. Correspondingly, the mutant c-myc proteins were resistant to Bz-423-induced degradation compared with wild-type transfected or endogenous c-myc protein. These results support a direct link between the reduction of c-myc and the antiproliferative response to Bz-423 and, along with the observed changes in cell cycle regulatory proteins, strongly indicate that the growth-inhibitory response is a result of c-myc depletion.

In addition to phosphorylation, T58 is a target for *O*-glycosylation by *O*-linked *N*-acetylglucosamine (46), and a dynamic interplay exists between *O*-glycosylation and phosphorylation of this residue (36). Because increased T58 phosphorylation or evidence for involvement of GSK-3β in Bz-423-induced degradation was not observed, it is possible that T58 glycosylation regulates Bz-423-induced c-myc proteasomal degradation. It is also possible that Bz-423 does not induce any specific T58 or S62 post-translational modifications but instead acts further downstream to increase the efficiency at which c-myc is processed by the proteasome. Rate-limiting steps in proteasomal degradation include both protein-specific modifications, such as phosphorylation, and the enzymatic attachment of ubiquitin to target proteins (47). Interestingly, reactive oxygen species stimulate cellular ubiquitin-ligase activity (48, 49). Therefore, Bz-423-induced O_2^- may enhance proteolytic processing of c-myc by increasing the expression and/or activity of specific ubiquitin ligases. In support of this possibility, we have observed recently that Bz-423 also induces the rapid, proteasome-dependent degradation of β-catenin (Supplementary Fig. S1), an oncogenic transcription factor that plays a critical role in Wnt signaling (50). However, Bz-423 does not alter expression of cyclin D1 and D2 (Fig. 2), indicating that some degree of specificity exists regarding which short-lived proteins are targeted following Bz-423 treatment.

In summary, this study identifies depletion of the oncogenic transcription factor c-myc as a key element in the mechanism leading G_1 arrest induced by the immunomodulatory benzodiazepine, Bz-423. The close connection between c-myc protein levels and neoplastic growth suggests that Bz-423 may have therapeutic potential against human neoplastic disease where deregulated c-myc expression underlies pathogenesis.

Acknowledgments

Received 9/28/2005; revised 11/11/2005; accepted 11/17/2005.

Grant support: NIH grants RO1 AI-47450 (G.D. Glick) and CA-48147 (A.W. Opipari, Jr.) and National Science Foundation Graduate Research Fellowship (T.B. Sundberg).

The costs of publication of this article were defrayed in part by the payment of page charges. This article must therefore be hereby marked *advertisement* in accordance with 18 U.S.C. Section 1734 solely to indicate this fact.

References

1. Pelengaris S, Khan M, Evan G. c-MYC: more than just a matter of life and death. Nat Rev Cancer 2002;2:764–6.
2. Atchley WR, Fitch WM. Myc and Max: molecular evolution of a family of proto-oncogene products and their dimerization partner. Proc Natl Acad Sci U S A 1995;92:10217–21.
3. Coller HA, Grandori C, Tamayo P, et al. Expression analysis with oligonucleotide microarrays reveals that MYC regulates genes involved in growth, cell cycle, signaling, and adhesion. Proc Natl Acad Sci U S A 2000;97:3260–5.
4. Gartel AL, Ye X, Goufman E, et al. Myc represses the p21(WAF1/CIP1) promoter and interacts with Sp1/Sp3. Proc Natl Acad Sci U S A 2001;98:45105.
5. Nesbit CE, Tersak JM, Prochownik EV. MYC oncogenes and human neoplastic disease. Oncogene 1999;18:3004–16.
6. Dang CV. c-Myc target genes involved in cell growth, apoptosis, and metabolism. Mol Cell Biol 1999;19:1–11.
7. Battey J, Moulding C, Taub R, et al. The human c-myc oncogene: structural consequences of translocation into the IgH locus in Burkitt lymphoma. Cell 1983;34:779–87.
8. Smith JB, Wickstrom E. Inhibition of tumorigenesis in a murine B-cell lymphoma transplant model by c-Myc complementary oligonucleotides. Adv Exp Med Biol 1998;451:17–22.
9. Huang Y, Snyder R, Kligshteyn M, Wickstrom E. Prevention of tumor formation in a mouse model of Burkitt's lymphoma by 6 weeks of treatment with anti-c-myc DNA phosphorothioate. Mol Med 1995;1:647–58.
10. Blatt NB, Bednarski JJ, Warner RE, et al. Benzodiazepine-induced superoxide signals B cell apoptosis: mechanistic insight and potential therapeutic utility. J Clin Invest 2002;110:1123–32.
11. Boitano A, Ellman JA, Glick GD, Opipari AW, Jr. The proapoptotic benzodiazepine Bz-423 affects the growth and survival of malignant B cells. Cancer Res 2003;63:6870–6.
12. Bednarski JJ, Warner RE, Rao T, et al. Attenuation of autoimmune disease in Fas-deficient mice by treatment with a cytotoxic benzodiazepine. Arthritis Rheum 2003;48:757–66.
13. Johnson KM, Chen X, Boitano A, Swenson L, Opipari AW, Jr., Glick GD. Identification and validation of the mitochondrial F(1)F(0)-ATPase as the molecular target of the immunomodulatory benzodiazepine bz-423. Chem Biol 2005;12:485–96.
14. Bunin BA, Plunkett MJ, Ellman JA. The combinatorial synthesis and chemical and biological evaluation of a 1,4-benzodiazepine library. Proc Natl Acad Sci U S A 1994;91:4708–12.
15. Djurhuus R. Ornithine decarboxylase (EC 4.1.1.17) assay based upon the retention of putrescine by a strong cation-exchange paper. Anal Biochem 1981;113:352–5.
16. Nitta T, Igarashi K, Yamamoto N. Polyamine depletion induces apoptosis through mitochondria-mediated pathway. Exp Cell Res 2002;276:120–8.
17. Chang BD, Watanabe K, Broude EV, et al. Effects of p21Waf1/Cip1/Sdi1 on cellular gene expression: implications for carcinogenesis, senescence, and age-related diseases. Proc Natl Acad Sci U S A 2000;97:4291–6.
18. Voigt W. Sulforhodamine B assay and chemosensitivity. Methods Mol Med 2005;110:39–8.
19. An S, Park MJ, Park IC, Hong SI, Knox K. Procaspase-3 and its active large subunit localized in both cytoplasm and nucleus are activated following application of apoptotic stimulus in Ramos-Burkitt lymphoma B cells. Int J Mol Med 2003;12:311–7.
20. Coffino P. Regulation of cellular polyamines by antizyme. Nat Rev Mol Cell Biol 2001;2:188–94.
21. Thomas T, Thomas TJ. Polyamines in cell growth and cell death: molecular mechanisms and therapeutic applications. Cell Mol Life Sci 2001;58:244–58.
22. Bello-Fernandez C, Packham G, Cleveland JL. The ornithine decarboxylase gene is a transcriptional target of c-Myc. Proc Natl Acad Sci U S A 1993;90:7804–8.
23. Murray AW. Recycling the cell cycle: cyclins revisited. Cell 2004;116:221–4.
24. Sherr CJ, Roberts JM. CDK inhibitors: positive and negative regulators of G_1-phase progression. Genes Dev 1999;13:1501–12.
25. Fernandez PC, Frank SR, Wang L, et al. Genomic targets of the human c-Myc protein. Genes Dev 2003;17:1115–29.
26. Cobrinik D. Pocket proteins and cell cycle control. Oncogene 2005;24:2796–809.

27. Zarkowska T, Mittnacht S. Differential phosphorylation of the retinoblastoma protein by G_1-S cyclin-dependent kinases. J Biol Chem 1997;272:12738–46.

28. Banerji L, Glassford J, Lea NC, Thomas NS, Klaus GG, Lam EW. BCR signals target p27(Kip1) and cyclin D2 via the PI3-K signalling pathway to mediate cell cycle arrest and apoptosis of WEHI 231 B cells. Oncogene 2001;20: 7352–67.

29. Alessi F, Quarta S, Savio M, et al. The cyclin-dependent kinase inhibitors olomoucine and roscovitine arrest human fibroblasts in G_1 phase by specific inhibition of CDK2 kinase activity. Exp Cell Res 1998; 245:8–18.

30. Zheng Y, Shi Y, Tian C, et al. Essential role of the voltage-dependent anion channel (VDAC) in mitochondrial permeability transition pore opening and cytochrome *c* release induced by arsenic trioxide. Oncogene 2004;23:1239–47.

31. Luscher B. Function and regulation of the transcription factors of the Myc/Max/Mad network. Gene 2001; 277:1–14.

32. Hu X, Bies J, Wolff L. Interferon β increases c-Myc proteolysis in mouse monocyte/macrophage leukemia cells. Leuk Res 2005;29:1307–14.

33. Chandramohan V, Jeay S, Pianetti S, Sonenshein GE. Reciprocal control of Forkhead box O 3a and c-Myc via the phosphatidylinositol 3-kinase pathway coordinately regulates p27Kip1 levels. J Immunol 2004;172:5522–7.

34. Sears R, Nuckolls F, Haura E, Taya Y, Tamai K, Nevins JR. Multiple Ras-dependent phosphorylation pathways regulate Myc protein stability. Genes Dev 2000; 14:2501–14.

35. Gregory MA, Hann SR. c-Myc proteolysis by the ubiquitin-proteasome pathway: stabilization of c-Myc in Burkitt's lymphoma cells. Mol Cell Biol 2000;20:2423–35.

36. Kamemura K, Hayes BK, Comer FI, Hart GW. Dynamic interplay between *O*-glycosylation and *O*-phosphorylation of nucleocytoplasmic proteins: alternative glycosylation/phosphorylation of THR-58, a known mutational hot spot of c-Myc in lymphomas, is regulated by mitogens. J Biol Chem 2002;277:19229–35.

37. Gregory MA, Qi Y, Hann SR. Phosphorylation by glycogen synthase kinase-3 controls c-myc proteolysis and subnuclear localization. J Biol Chem 2003;278: 51606–12.

38. Rajkumar SV, Richardson PG, Hideshima T, Anderson KC. Proteasome inhibition as a novel therapeutic target in human cancer. J Clin Oncol 2005;23:630–9.

39. Coghlan MP, Culbert AA, Cross DA, et al. Selective small molecule inhibitors of glycogen synthase kinase-3 modulate glycogen metabolism and gene transcription. Chem Biol 2000;7:793–803.

40. Prochownik EV. c-Myc as a therapeutic target in cancer. Expert Rev Anticancer Ther 2004;4:289–302.

41. Hermeking H. The MYC oncogene as a cancer drug target. Curr Cancer Drug Targets 2003;3:163–75.

42. Berg T, Cohen SB, Desharnais J, et al. Small-molecule antagonists of Myc/Max dimerization inhibit Myc-induced transformation of chicken embryo fibroblasts. Proc Natl Acad Sci U S A 2002;99:3830–5.

43. Yin X, Giap C, Lazo JS, Prochownik EV. Low molecular weight inhibitors of Myc-Max interaction and function. Oncogene 2003;22:6151–9.

44. Oster SK, Mao DY, Kennedy J, Penn LZ. Functional analysis of the N-terminal domain of the Myc oncoprotein. Oncogene 2003;22:1998–2010.

45. Yeh E, Cunningham M, Arnold H, et al. A signalling pathway controlling c-Myc degradation that impacts oncogenic transformation of human cells. Nat Cell Biol 2004;6:308–18.

46. Chou TY, Dang CV, Hart GW. Glycosylation of the c-Myc transactivation domain. Proc Natl Acad Sci U S A 1995;92:4417–21.

47. Ang XL, Wade Harper J. SCF-mediated protein degradation and cell cycle control. Oncogene 2005;24: 2860–70.

48. Li YP, Chen Y, Li AS, Reid MB. Hydrogen peroxide stimulates ubiquitin-conjugating activity and expression of genes for specific E2 and E3 proteins in skeletal muscle myotubes. Am J Physiol Cell Physiol 2003;285: C806–12.

49. Jahngen-Hodge J, Obin MS, Gong X, et al. Regulation of ubiquitin-conjugating enzymes by glutathione following oxidative stress. J Biol Chem 1997;272:28218–26.

50. Luu HH, Zhang R, Haydon RC, et al. Wnt/β-catenin signaling pathway as a novel cancer drug target. Curr Cancer Drug Targets 2004;4:653–71.